Advanced Modified Direct Torque Control with Space Vector Modulation Based on Active Disturbance Rejection Control for Induction Motor Sensorless Drive

Chalawane Haitam
ENSET University MOHAMMED V, Electrical Engineering
Research Laboratory, Rabat, Morocco
Email: chalawanehaitam@gmail.com

Essadki Ahmed and Nasser Tamou
ENSET, ENSIAS,
University MOHAMMED V, Rabat, Morocco
Email:{ahmed.essadki1,tamounasser}@gmail.com

***Abstract*—This work addresses the problems inherent in the disturbances affected to the operation of electrical motor drives, a modified direct torque control which is among the excellent method of torque control of an induction motor that provide a decoupled control of flux and torque is implemented with a novel controller of active disturbance rejection controller to cancel the drawbacks of flux ripples, high torque at start-up and also variable switching frequency associated in the classical DTC. In the other side, an advanced estimator for rotor speed is used in order to rectify the problem of sensors. The proposed control strategy, implementation data, and simulations with MDTC are presented and discussed. It is concluded that MDTC-SVM proposed control topology offers high performance in steady-state operation despite the existence of the internal and external disturbances.**

***Index Terms*—Induction motor, modified direct torque control, fuzzy logic control, active disturbance dejection control.**

NOMENCLATURE

ω_r	Rotor speed
p	Number of pole pairs
η	Inverse of rotor time constant
M, L_s, L_r	Magnetizing, stator and rotor inductance
R_s, R_r	Stator and rotor resistance
$x, \hat{x}$	Real and estimated value of x
i_d, i_q	Currents in stationary reference frame
v_d, v_q	Voltages in stationary reference frame
ψ_{rd}, ψ_{rq}	Rotor fluxes in stationary reference frame
ψ_{sd}, ψ_{sq}	Stator fluxes in stationary reference frame

Manuscript received July 7, 2018; revised July 25, 2019.

I. INTRODUCTION

In the last decade, it found birth a new control topologies of the torque control mostly the Direct Torque Control (DTC) that was presented by Takahashi and T. Noguchi, this approach has been introduced in order to control the induction motor, more precisely for decoupling the torque and flux.

Direct torque control is composed of a lookup table, torque and flux calculators, a voltage-source inverter (VSI), and a pair of hysteresis comparators, and presents some influential problems on the induction motor operation, such as high torque and flux ripples with current distortion, the changes of switching frequency owing to operating conditions [2].

Recently, In the first years of the new decade the authors of the new command strategy have been incessantly developed and enhanced the control because of many disadvantages faced in the classical DTC. To make the control more suitable, cancelling the drawbacks which are aforementioned, keeping the simplicity of the classical DTC and certainly improve the steady state performance of an induction motor, this work presents an advanced technique of modified direct torque control using active disturbance rejection controller [11].
Thence, the space vector modulation (SVM) strategy was implemented with DTC scheme (DTC-SVM) because it produces less total harmonic distortion THD during operation. Multiple SVM strategy were introduced in the literature, such as highest current non-switched sequence, right aligned sequence, alternating zero vector sequence and symmetrical sequence [3].

Since the induction motor drives are imposed with nonlinear characteristics, the researchers developed a new command to deal with these problems called Active Disturbance Rejection Control (ADRC) that was introduced by Han in 1998 and created for nonlinear system, its significant advantage is it may estimate and compensate the parameter variations as the external disturbances. accordingly, it does not require the accurate model of the plant. In other words, the design of ADRC is independent of the controlled system model and its parameters [9].

In this work, the MRAS estimator is presented, the implementation of both flux and rotor speed in closed-loop becomes easy. This paper is organized as follows: Section 2 describes the proposed Modified Direct Torque Control. Section 3 presents the Active Disturbance Rejection Control. Section 4 introduces the proposed Model Reference Adaptive System for speed estimation. Section 5 deals with the simulation results. Finally, conclusions are given in Section 6.

II. Proposed Direct Torque Control

In general, an engine with symmetric induction in three phases, the instantaneous electromagnetic torque is based on the product of the rotor flux linkage space vector and the stator flux linkage space vector and presented as follows:

$$T_e = (3p/2)|\psi_s||\psi_r'|\sin\delta \tag{1}$$

Whereabouts, $|\psi_r'|$ presents the rotor flux linkage space vector referred to stator, $\psi_s$is the stator flux linkage space vector, p is the number of pole pairs and finally δ is the angle between the stator and rotor flux linkage space vector [8].

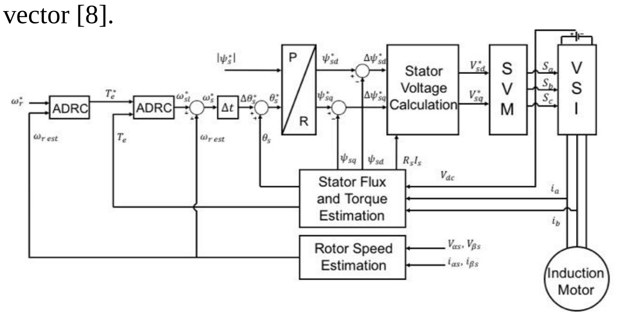

Figure 1. Block diagram of proposed MDTC.

Fig. 1 shown above introduces the structure of proposed MDTC applied on induction motor. So, instead of using voltage-switching table and the hysteresis comparators of conventional DTC, we implement a SVPWM technique and calculation of the reference of voltage space vector. By dint of this strategy and maintaining the constant amplitude of reference stator flux, the torque control is achieved.

The instantaneous electromagnetic torque presented in equation (5) is achieved by controlling torque angle change and keeping the rotor and stator flux vectors at constant amplitude. Then, with same principle applied in [5] and [6], (1) torque equation is replaced by the following equation of (2) [5]:

$$T_e(t) = \left[\frac{3}{2}p\frac{M^2}{R_r {L_s}^2}\left|{\psi_s}^2\right|\right]\left[1-e^{-\frac{t}{\tau}}\right]\ (\omega_s-\omega_r) \tag{2}$$

The time constant τ is given as: $\tau = \sigma L_r/R_r$

The term of $(\omega_s-\omega_r)$ presents the slip angular frequency ω_{slip}, the slip between rotor angular frequency ω_r and the stator flux angular frequency ω_s and can be presented as:

$$\omega_{slip} = \omega_s - \omega_r \tag{3}$$

Then, by substituting Equation (3) into (2), we obtain the following equation of electromagnetic torque:

$$T_e(t) = \left[\frac{3}{2}p\frac{M^2}{R_r {L_s}^2}\left|{\psi_s}^2\right|\right]\left[1-e^{-\frac{t}{\tau}}\right](\omega_{slip}) \tag{4}$$

Afterward, it's clear that the instantaneous electromagnetic torque is proportional to slip angular frequency, which can be rewritten as:

$$\omega_{slip} = \frac{d\theta_{slip}}{dt} = \frac{\Delta\theta_{slip}}{\Delta t} \tag{5}$$

Where the sampling time θ_{slip} is the angle between stator flux vector axis and rotor axis. Finally, the modified instantaneous electromagnetic torque is given by substituting equation (5) into (4):

$$T_e(t) = \left[\frac{3}{2}p\frac{M^2}{R_r {L_s}^2}\left|{\psi_s}^2\right|\right]\left[1-e^{-\frac{t}{\tau}}\right]\left(\frac{\Delta\theta_{slip}}{\Delta t}\right) \tag{6}$$

A. Direct Stator Flux Control Method

Applying a direct stator flux control technique, the changing value of slip angle $\Delta\theta_{slip}$ is controlled and can be performed in the instantaneous electromagnetic torque [4]. The main objective in stator flux control technique is decoupling the amplitude and angle of stator flux vector. From the above block diagram Fig.1, reference torque is generated from speed ADRC controller [7].

In order to compensate the torque error ΔT_e between the estimated real torque and reference torque, the angle of stator flux linkage must be increased from θ_s to $\theta_s + \Delta\theta_s$ as presented in phase diagram in Fig. 2, and $\Delta\theta_s = \Delta\theta_{sl}$, thus:

$$\theta_s^* = \theta_s + \Delta\theta_{sl} \tag{7}$$

where $\Delta\theta_{sl}$ is the change in slip angle, it is found as($\theta_{sl} = \int \omega_{sl}\, dt$), and generated from torque ADRC regulator.

Afterwards, the required reference stator flux vector in polar form is given by:

$$\psi_s^* = |\psi_s^*|\angle\theta_s^* \tag{8}$$

θ_s^* is the angle of the reference stator flux and calculated from equation (7), $|{\psi_s}^*|$ keep constant at rated value. Therefore, required slip angel is written by:

$$\Delta\theta_{sl} = \omega_{slip}\Delta t \tag{9}$$

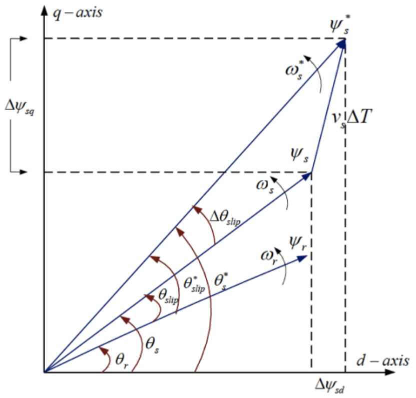

Figure 2. Control of stator flux linkage.

The reference flux vector is given by:

$$\psi_{sd}^{*} = \psi_{s}^{*}\cos(\theta_{s}^{*}) \tag{10}$$

$$\psi_{sq}^{*} = \psi_{s}^{*}\sin(\theta_{s}^{*}) \tag{11}$$

Estimated actual flux magnitude is:

$$\psi_{sd} = \int (V_{sd} - i_{sd}R_s)\,dt \tag{12}$$

$$\psi_{sq} = \int (V_{sq} - i_{sq}R_s)\,dt \tag{13}$$

The flux error is given by:

$$\Delta\psi_{sd} = \psi_{sd}^{*} - \psi_{sd} \tag{14}$$

$$\Delta\psi_{sq} = \psi_{sq}^{*} - \psi_{sq} \tag{15}$$

For both cases, $\Delta\psi_s$ is the flux error between reference flux and estimated actual flux.

The reference space voltage vector is given by:

$$V_{sd}^{*} = \Delta\psi_{sd}/\Delta t + i_{sd}R_s \tag{16}$$

$$V_{sq}^{*} = \Delta\psi_{sq}/\Delta t + i_{sq}R_s \tag{17}$$

With Δt is the sampling time.

Time signals are calculated and generate the pulses to control the voltage source inverter as explained in [6].

III. Proposed Control Strategy

Owing to the nonlinearity and complexity of the electrical power system, the researchers have tried to find a way to design a powerful controller in order to obtain better control performance. Therefore, the active disturbance rejection control (ADRC) strategy which is presented and implemented in this work, is designed to remedies the disadvantages of nonlinear PID control and inherits its advantages simultaneously. Additionally, the control becomes a more robust and effective for uncertain systems and equally presents a high precision in terms of the influence of external and internal disturbance due to the extended state observer, the basic element and a powerful anti-disturbance of ADRC. The third-order LADRC structure is presented in Figure 4 and the controlled process is followed by (18) [1] [9]:

$$\ddot{y} = bu + f(\dot{y}, y, u, d) \tag{18}$$

where u and y are respectively the input and the output of the system, f denotes the total disturbance including external disturbance and internal disturbance, b is a constant and denotes the process parameter [12].

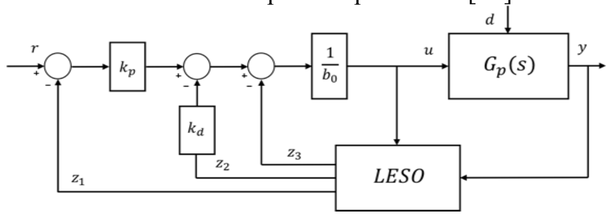

Figure 3. The linear ADRC structure.

Finally, d denotes the system external disturbance. The state space equation is presented in the following:

$$\begin{cases} x_1' = x_2 \\ x_2' = x_3 + b_0 u \\ x_3' = \dot{f} \\ y = x_1 \end{cases} \tag{19}$$

The linear extended state observer (LESO) in the following (25) in order to estimate the value of $y, \dot{y}$ and f [9].

$$\begin{cases} z_1' = z_2 + \beta_1(y - z_1) \\ z_2' = z_3 + \beta_2(y - z_1) + b_0 u \\ z_3' = \beta_3(y - z_1) \end{cases} \tag{20}$$

Then, the parameters of observer gain are presented in [9] as follows:

$$[\beta_1, \beta_2, \beta_3] = [3\omega_0, 3\omega_0^2, 3\omega_0^3] \tag{21}$$

where ω_0 is the observer bandwidth. In the duration of parameters tuning process, z_1, z_2, z_3 should track y, $\dot{y}$, f respectively and the disturbance compensation is as follows:

$$u = \frac{u_0 - z_3}{b_0} \tag{22}$$

So, the control system is converted into an integral cascade as shown below in (23):

$$\ddot{y} = f + u_0 - z_3 \approx u_0 \tag{23}$$

At that time, the Proportional derivative control law is given as:

$$u_0 = k_p(r - z_1) - k_d z_2 \tag{24}$$

With:

$$k_p = \omega_c^2 \; and \; k_d = 2\omega_c \tag{25}$$

where ω_c is the PD bandwidth, the equation (6) presented in the previous section can be achieved as:

$$T_e = \frac{B_M}{1 + \tau s} * \left(\frac{\Delta\theta_{slip}}{\Delta t}\right) \tag{26}$$

Where $B_M = \frac{3}{2} p \frac{M^2}{R_r {L_s}^2} |{\psi_s}^2|$ is constant.

The expression of the electromagnetic torque can be given into the form:

$$\dot{T}_e = \frac{B_M}{\tau.\Delta t} * \Delta\theta_{slip} - \frac{1}{\tau} * T_e \tag{27}$$

Then, we can deduce the following equation according to ADRC form:

$$\frac{dT_e}{dt} = f(T_e, d, t) + b_0 u(t) \tag{28}$$

Where:

$$\begin{cases} f = -\dfrac{1}{\tau} * T_e + \left(\dfrac{B_M}{\tau.\Delta t} - b_0\right) * \Delta\theta_{slip} \\ u = \Delta\theta_{slip} \quad b_0 = \dfrac{B_M}{\tau.\Delta t} \end{cases} \tag{29}$$

f represents the total disturbance affecting the electromagnetic torque T_e , b_0 is the parameter gain to approximate, $u = \Delta\theta_{slip}$ is the control input of the torque loop T_e. Finally, choosing a suitable response time, we can obviously determine the parameters k_p and k_d of the ADRC controller.

IV. Proposed MRAS Observer

In this subsection, the model reference adaptive method (MRAS) is presented. Depending on the principle of direct torque controlling of sensorless induction motor, getting the angle and amplitude of the rotor flux is one of the most influential factors affecting the performance of the system control.

A. Reference Model

The reference model generates the reference value of the rotor flux components in the stationary reference frame (α, β). The reference rotor flux components obtained from the reference model are given by:

$$\frac{d}{dt}\Phi_{\alpha r} = \frac{L_r}{M}\left(V_{\alpha s} - R_s i_{\alpha s} - \sigma L_s \frac{d}{dt} i_{\alpha s}\right) \tag{30}$$

$$\frac{d}{dt}\Phi_{\beta r} = \frac{L_r}{M}\left(V_{\beta s} - R_s i_{\beta s} - \sigma L_s \frac{d}{dt} i_{\beta s}\right) \tag{31}$$

B. Adaptive Model

The adjustable model is designed using the rotor equations, this observer estimates both the fluxes and the speed. The equations of the observer are formed as follows:

$$\begin{cases} \dfrac{d}{dt}\hat{\psi}_\alpha = -\eta\hat{\psi}_\alpha - p\widehat{\omega}_r\hat{\psi}_\beta + \eta M i_\alpha \\ \dfrac{d}{dt}\hat{\psi}_\beta = p\widehat{\omega}_r\hat{\psi}_\alpha - \eta\hat{\psi}_\beta + \eta M i_\beta \end{cases} \tag{32}$$

$$\begin{cases} \widehat{\omega}_r = M.sign(s) \\ s = \psi_\beta\hat{\psi}_\alpha - \psi_\alpha\hat{\psi}_\beta \end{cases} \tag{33}$$

The equation (33) represents the discontinuous estimated speed, manifold s is differentiated, constructed as a combination of the reference fluxes ψ_α ,ψ_β and the estimated fluxes $\widehat{\psi}_\alpha$, $\widehat{\psi}_\beta$ and is presented in the following form :

$$\dot{s} = p\omega_r(\psi_\alpha\hat{\psi}_\alpha + \psi_\beta\hat{\psi}_\beta) + 2\eta(\psi_\alpha\hat{\psi}_\beta - \hat{\psi}_\alpha\psi_\beta) + \eta M[(\hat{\psi}_\alpha - \psi_\alpha)i_\beta - (\hat{\psi}_\beta - \psi_\beta)i_\alpha] - p(\hat{\psi}_\alpha\psi_\alpha + \hat{\psi}_\beta\psi_\beta)\widehat{\omega}_r \tag{34}$$

With the assumption of that the adjustable model converges and $\widehat{\psi}_\alpha \to \psi_\alpha$, $\widehat{\psi}_\beta \to \psi_\beta$, the coefficient of $\widehat{\omega}_r$ becomes as following $p(\widehat{\psi}_\alpha\psi_\alpha + \widehat{\psi}_\beta\psi_\beta) = p\psi^2 > 0$ and the equation (34) can be rewritten as:

$$\dot{s} = f - p\psi^2 M.sign(s) \tag{35}$$

If $s = 0$, it can equally be assumed that $\dot{s} = 0$ and the equivalent control of $\widehat{\omega}_r$ represents the low frequency component of the switching term $M.sign(s)$ [5]-[6] and given as:

$$\omega_{r,eq} = \omega_r + \frac{\eta M[(\hat{\psi}_\alpha - \psi_\alpha)i_\beta - (\hat{\psi}_\beta - \psi_\beta)i_\alpha] + 2\eta(\hat{\psi}_\beta\psi_\alpha - \hat{\psi}_\alpha\psi_\beta)}{\hat{\psi}_\alpha\psi_\alpha + \hat{\psi}_\beta\psi_\beta} \tag{36}$$

The numerator of the second term shown in (36) becomes equal to zero when the adjustable model observer converges. Thus, it is obvious that $\omega_{r,eq} \to \omega_r$ and is obtained by low pass filtering the switching term $M.sign(s)$ and represents the estimated speed of the observer.

Using a second-order sliding mode technique, the switching term $\widehat{\omega}_r$ is redesigned as:

$$\widehat{\omega}_r = \alpha\sqrt{|s|}\,sign(s) + \beta\int(sign(s)) \tag{37}$$

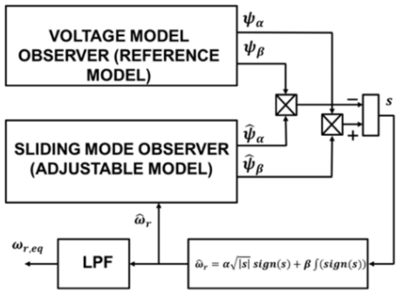

Figure 4. Block diagram of proposed MRAS.

The simulation, $\alpha = 1352$; $\beta = 561$. A compromise value of α should be found, neither too small nor too higher to get an improved quality of the speed with accurate estimate during transients.

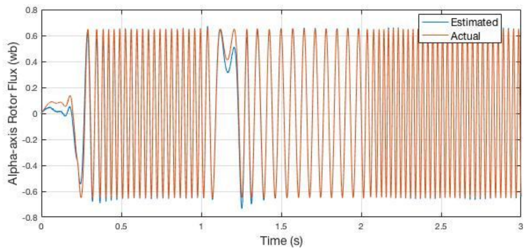

(a)

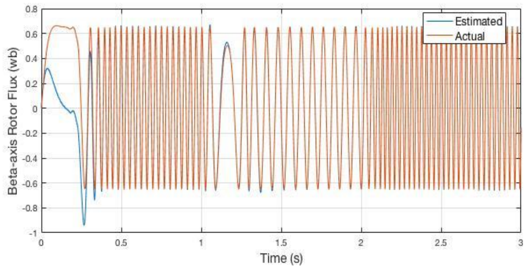

(b)

Figure 5. A comparison between the actual rotor fluxes of IM and the estimated of MRAS (a), Alpha-axis rotor flux (b), Beta-axis rotor flux.

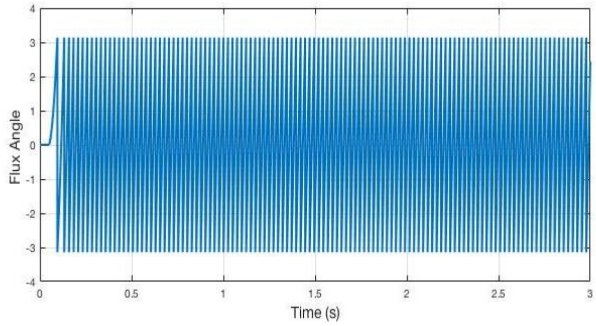

Figure 6. Flux angle of proposed MRAS.

Fig.5 and Fig.6 present the fluxes results in alpha-beta reference frame of the proposed MRAS. As shown in above figures, the actual fluxes track the reference with a little overshoot at start-up, it concluded that the proposed MRAS introduces an acceptable result in order to generate the desired rotation speed.

V. Simulation Results and Discussions

The performance of the both system "Command+Estimator " in perturbation rejection and trajectory tracking shown in these figures, is evaluated under a variety of operating conditions such as the changes of motor drive parameters, an abrupt variation in speed control and for step change in load.

In order to study the robustness limit of the proposed command, the responses are obtained under rotor resistance variation R_r that varies until 60%.

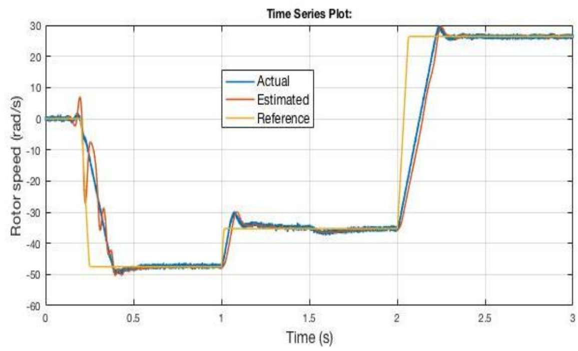

Figure 7. Rotor speed of IM.

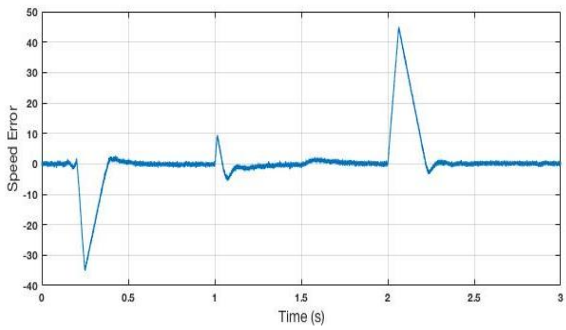

Figure 8. The error of the estimated and reference speed.

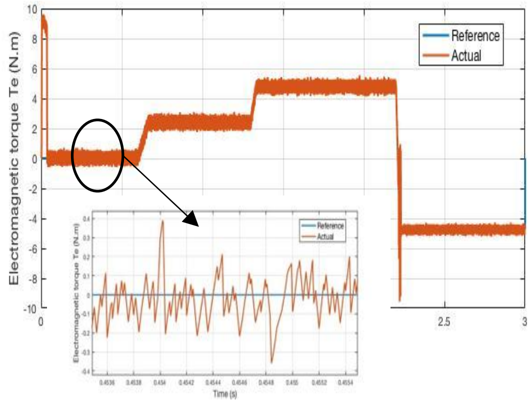

Figure 9. Electromagnetic torque of IM.

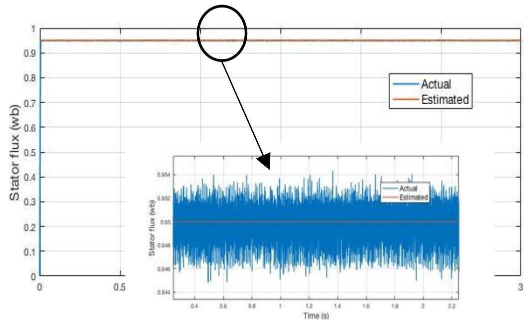

Figure 10. Stator flux of induction motor.

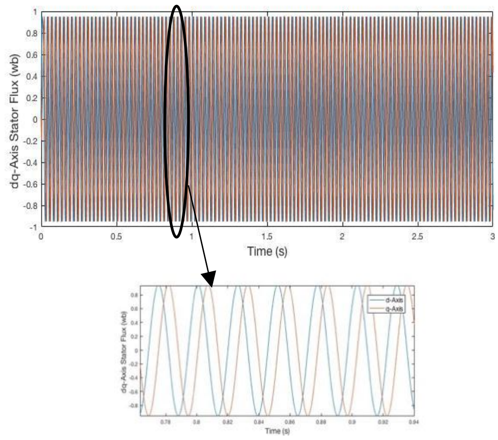

Figure 11. D-q axis stator flux of induction motor.

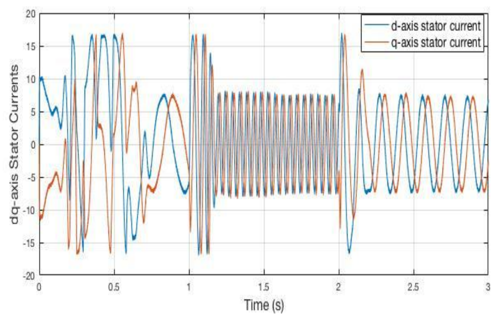

Figure 12. D-q axis stator currents of induction motor.

Fig.12 demonstrates the capability of the proposed system is verified when the stator currents are obviously circular and its trajectory is almost sinusoidal. As shown in Fig. 7, a sudden speed change from -50 to 27 rad/s, varying load torque to the following values (2, 6, 4.2) N.m, and the motor speed tracks the reference with a little overshoot. Fig. 8 introduces the error speed between the estimated and the reference speed. Fig. 10 presents the stator flux of the induction motor that tracks the reference at 0.95 wb and Fig. 11 shows the stator flux in the d-q axis reference frame. Fig. 9 presents the electromagnetic torque comparing the reference and the actual torque of induction motor.

In terms of perturbation rejection, we notice that proposed ADRC control rejects rapidly the load disturbance with a negligible steady state error except at the time when the load is suddenly changed, the previous figures show the efficiency of the control system. In terms of trajectory tracking, the validity of the speed estimator structure assured by MATLAB/Simulink simulations is used as feedback in the closed loop, then in some figures that introduce the estimated, actual and reference values and errors are presented, and we notice that the actual and estimated motor speed converge to the reference speed. In spite of that, it appears a small static error when the motor speed varies.

Comparing the waveforms, using the proposed technique produces the reduction of the ripple and overshoot is obtained related to conventional switching table technique of DTC. Finally, high tracking accuracy is observed at all speed, rejection of external and internal disturbances could be realized and the response time is enhanced.

VI. Conclusion

This paper has introduced an advanced modified Direct Torque Control with space vector modulation based on active disturbance rejection control(ADRC), Using MDTC-SVM strategy, the real switching frequency becomes constant and controllable, Afterward, the total harmonic disturbance of the flux, torque and currents is minimized by the implementation of extended state observer (ESO) which is the significant element of ADRC. Then, it concluded that the performance of the proposed scheme is superior in terms of robustness to parameters variation as rotor and stator resistances and consequently, the system presents less ripples. On the other hand, an enhanced MRAS speed estimator based on the rotor flux estimation was presented and implemented at low and high speeds.

Appendix

ADRC controller parameters:
The direct current gains of stator:

$$\beta_{1d} = 620\ ;\ \beta_{2d} = 231$$

The quadrature current gains of stator:

$$\beta_{1q} = 250\ ;\ \beta_{2q} = 4.10^{-3}$$

Stator currents controller gain k_{p-s}= *170*
Stator currents parameter b_{so}= *113*

TABLE I. IM Drive Parameters

Symbol	Quantity	Numerical application
f	Current stator frequency	50 Hz
p	Number of pole pairs	2
J	Moment of inertia	0.029 Kg.m ²
Rs	Stator resistance	4.85 Ω
Rr	Rotor resistance	3.7 Ω
M	Mutual inductance	0.265 H
Ls	Stator inductance	0.315 H
Lr	Rotor inductance	0.315 H
Nn	rated speed	27 rad/sec
U	Power supply voltage	380 V

References

[1]. Xiao and B. Yan, “Improved linear active disturbance rejection control for microgrid frequency regulation,” *Energies,* vol. 10, no. 7, 2017, pp.1047.

[2]. Chintala, R. Lokeshwar, S. K. Peddapelli, and S. Malaji, “Improvement in performance of cascaded multilevel inverter using triangular and trapezoidal triangular multi carrier SVPWM,” *AEEE,* vol. 14, no. 5, p. 562, 2016.

[3]. A. H. Abosh, Z. Q. Zhu, and Y Ren, “Reduction of torque and flux ripples in space vector modulation-based direct torque control of asymmetric permanent magnet synchronous machine,” *IEEE Transactions on Power Electronics*, vol. 32, no. 4, pp. 2976-2986, 2017.

[4]. V. Kumar and S. Rao, “Modified direct torque control of three-phase induction motor drives with low ripple in flux and torque,” *Leonardo Journal of Sciences*, vol. 10, no. 18, pp. 27-44, 2011.

[5]. Y. Kumsuwan, S. Premrudeepreechacharn, and H. A Toliyat, “Modified direct torque control method for induction motor drives based on amplitude and angle control of stator flux,” *Electric Power Systems Research*, vol. 78, no. 10, pp. 1712-1718, 2008.

[6]. A. Kumar, B. G. Fernandes, K. Chatterjee, “Simplfied svmpwm-dtc of three phase induction motor using the concept of imaginary switching times,” *in Conference Proc. the 30th Annual Conference of the IEEE Industrial Electronics Society,* November 2-6, Busan, Korea, 2004.

[7]. L. Tang, L. Zhong, M. F. Rahman, Y. Hu, “A novel direct torque controlled interior permanent magnet synchronous machine drive with low ripple in flux and torque and fixed switching frequency,” *IEEE Transactions on Power Electronics,* vol. 19, no. 2, pp. 346-354, 2004.

[8]. L. Tang, L. Zhong, F. Rahman, “Modelling and experimental approach of a novel direct torque control scheme for interior permanent magnet synchronous machine drive,” in *Proc. IEEE IECON’02*, Seville, Spain, 2002, 1, pp. 235-240.

[9]. C. Haitam, E. Ahmed, and N.Tamou, “DTC-SVM based on active disturbance rejection control applied on sensorless induction motor,” in *Proc. ICSDE,* pp. 127-133, 2017, July, ACM.

[10]. Zadeh, A. Lotfi, “Fuzzy sets,” *Information and Control, vol.* 8, no. 3, pp. 338-353, 1965.

[11]. Abosh, H. Atheer, Z. Q. Zhu, and Y. Ren, “Cascaded direct torque control of unbalanced PMSM with low torque and flux ripples,” *IEEE Transactions on Power Electronics,* 2017.

[12]. H. Chalawane, A. Essadki, and N. Nasser, “Influence of increasing stator resistance on active disturbance rejection control based sensorless induction motor compared with to conventional PI and fuzzy logic control,” *International REview of Automatic Control (IREACO*), vol. 11, no. 5, 2018.

Haitam Chalawane received a Master degree in 2014 From High School of Technical Education ENSET, Mohammed V University, Rabat. He is currently working toward the Ph.D. degree in electrical engineering research at the electrical engineering department of ENSET, His major research interests are the advanced control techniques for electrical machines and drives.

Ahmed Essadki is currently a Professor and university research professor at the electrical engineering department of ENSET, Mohammed V University, Morocco. In 2000, He received his PhD degree from Mohammadia Engineering School (EMI), (Morocco). From1990 to 1993, he pursued his Master program at UQTR University, Quebec Canada, respectively, all in electrical engineering. His current research interests include renewable energy, motor drives and power system. Doctor Ahmed Essadki is a member of RGE Lab in research group leader.

Tamou Nasser is currently an Associate Professor at the communication networks department of National High School for Computer Science and Systems (ENSIAS), Mohammed V University, Morocco, since 2009. She received her PhD degree in 2005 and her research MS degree, in 2000, respectively, all in electrical engineering from Mohammadia Engineering School (EMI), Morocco. Her research interests are renewable energy, motor drives, power system, she is a member of Al Jazari research group.